UCLA
UCLA Previously Published Works

Title

Associations between hippocampal morphometry and neuropathologic markers of Alzheimer's disease using 7T MRI

Permalink

https://escholarship.org/uc/item/6r73k37s

Authors

Blanken, Anna E
Hurtz, Sona
Zarow, Chris
et al.

Publication Date

2017

DOI

10.1016/j.nicl.2017.04.020

Peer reviewed

CrossMark
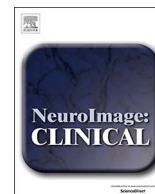
Associations between hippocampal morphometry and neuropathologic markers of Alzheimer's disease using 7 T MRI

Anna E. Blanken[a], Sona Hurtz[b], Chris Zarow[c], Kristina Biado[d], Hedieh Honarpisheh[e], Johanne Somme[f], Jenny Brook[g], Spencer Tung[d], Emily Kraft[h], Darrick Lo[d], Denise W. Ng[d], Harry V. Vinters[d], Liana G. Apostolova[i,j,]*

[a] Department of Psychology, University of Southern California, Los Angeles, CA, USA
[b] Drexel University College of Medicine, Philadelphia, PA, USA
[c] Department of Neurology, Keck School of Medicine at the University of Southern California, Los Angeles, CA, USA
[d] Department of Pathology & Laboratory Medicine, UCLA, Los Angeles, CA, USA
[e] Department of Pathology, University of Texas MD Anderson Cancer Center, Houston, TX, USA
[f] Department of Neurology, Barakaldo, Basque Country, Spain
[g] Department of Medicine - Statistics Core, UCLA, Los Angeles, CA, USA
[h] University of Rochester, Rochester, N.Y, USA
[i] Department of Neurology, David Geffen School of Medicine, University of California Los Angeles, Los Angeles, CA, USA
[j] Department of Neurology, Indiana University School of Medicine, Indianapolis, IN, USA

ARTICLE INFO

ABSTRACT

Hippocampal atrophy, amyloid plaques, and neurofibrillary tangles are established pathologic markers of Alzheimer's disease. We analyzed the temporal lobes of 9 Alzheimer's dementia (AD) and 7 cognitively normal (NC) subjects. Brains were scanned post-mortem at 7 Tesla. We extracted hippocampal volumes and radial distances using automated segmentation techniques. Hippocampal slices were stained for amyloid beta (Aβ), tau, and cresyl violet to evaluate neuronal counts. The hippocampal subfields, CA1, CA2, CA3, CA4, and subiculum were manually traced so that the neuronal counts, Aβ, and tau burden could be obtained for each region. We used linear regression to detect associations between hippocampal atrophy in 3D, clinical diagnosis and total as well as subfield pathology burden measures. As expected, we found significant correlations between hippocampal radial distance and mean neuronal count, as well as diagnosis. There were subfield specific associations between hippocampal radial distance and tau in CA2, and cresyl violet neuronal counts in CA1 and subiculum. These results provide further validation for the European Alzheimer's Disease Consortium Alzheimer's Disease Neuroimaging Initiative Center Harmonized Hippocampal Segmentation Protocol (HarP).

1. Introduction

More than 5 million Americans are currently living with Alzheimer's disease (AD). AD is the 6th leading cause of death in the United States and the most common neurodegenerative disorder worldwide. As we experience growing populations and increasing life expectancies, we will soon see a dramatic spike in the prevalence of AD. In the hands of highly trained dementia specialists, the accuracy of bedside clinical diagnosis is still suboptimal, reaching 70.9% to 87.3% sensitivity and 44.3% to 70.8% specificity (Beach et al., 2012; Shim et al., 2013). Thus post-mortem examination of brain abnormalities remains as the gold standard for AD diagnosis.

The main pathologic indicators of AD are amyloid plaques and neurofibrillary tangles. Amyloid plaques are crucial for the diagnosis of AD and are made up of amyloid protein (Aβ). However, amyloid plaques alone do not correlate with cognitive decline in dementia. Aβ in AD tends to spread first through the neocortex and then the limbic structures, such as the hippocampus (Thal et al., 2000). Neurofibrillary tangles contain hyperphosphorylated tau protein and are commonly seen in neurodegenerative disorders (Braak and Braak, 1991, 1997). They have been associated with cortical and hippocampal atrophy in AD (Nelson et al., 2012). Tau tends to collect first in entorhinal areas, and then spread to the subiculum, CA1, CA2, and CA3 areas of the hippocampus, followed by the neocortex (Arnold et al., 1991; Bobinski et al., 1995; Schonheit et al., 2004).

The hippocampus is one of the first brain regions to show the effects

of AD pathology and, consequently, atrophy of the hippocampal structures is the most established neurodegenerative imaging biomarker of AD (Apostolova et al. 2006b; Apostolova et al., 2006c; Apostolova et al., 2010b; Hof et al., 1996; Jack et al., 2002). In most imaging studies the average hippocampal volume, which can be relatively easily extracted from magnetic resonance imaging (MRI) data, is compared between study groups.

Recently, neuroimaging techniques have allowed for 3D modeling of hippocampal changes and have been valuable for the longitudinal study of neuropathologic changes in AD (Apostolova et al., 2006c; Apostolova et al., 2010a; Duchesne et al., 2015). The present study uses a computational anatomy shape-based method called hippocampal radial distance in order to compare cross-sectional 3D hippocampal maps of subjects diagnosed with dementia and normal controls. This technique allows for detection of subtler hippocampal shape changes in AD (Apostolova et al., 2006a; Apostolova et al., 2006c; Apostolova et al., 2012; Apostolova et al., 2010b; Frisoni et al., 2006; Thompson et al., 2004). The hippocampal radial distance approach relies on manual or automated hippocampal segmentations, which are converted into 3D anatomical mesh models for each subject. The distance from a center core of the 3D structure to each surface point (i.e., the radial distance) is computed and plotted onto the surface. As the disease progresses and the hippocampus atrophies, the radial distance shrinks. Compared to the conventional region of interest (ROI) technique, which extracts hippocampal volumes - a single summary metric - from each hippocampus, our technique allows for visualization of differences between diagnostic groups in cross-sectional studies (Apostolova et al., 2010a; Morra et al., 2009), or changes over time in longitudinal studies (Apostolova et al., 2010a; Morra et al., 2009). The results presented here provide further validation of the radial distance mapping technique.

The European Alzheimer's Disease Consortium (EADC) and the Alzheimer's Disease Neuroimaging Initiative (ADNI) developed the EADC-ADNI Harmonized Hippocampal Segmentation Protocol (HarP) (Frisoni and Jack, 2011) in order to reduce the significant variation in hippocampal volumetric estimates among existing hippocampal segmentation protocols (Boccardi et al., 2011). Investigators in the EADC-ADNI HarP group examined, operationalized, and quantified the differences in 12 different hippocampal segmentation protocols (Boccardi et al., 2014), and reached a consensus among a group of international hippocampal segmentation experts using an iterative Delphi procedure, thereby establishing a final protocol (Boccardi et al., 2015). Five expert tracers established a "gold standard" for hippocampal traces used to train naïve tracers and validate the protocol (Bocchetta et al., 2015; Frisoni et al., 2015).

Ex vivo high resolution MRI has allowed for in depth exploration of brain structures such as the hippocampus. The hippocampus is comprised of several subfields including the dentate gyrus, subiculum, and cornu ammonis subfields 1–4 (CA1, CA2, CA3, and CA4). Few studies have investigated unique relationships of hippocampal subfields to the progression of AD pathology in the brain. Some studies have reported subregion-specific hippocampal atrophy related to the presence and spread of neurofibrillary tangles in the hippocampal structures (Greene and Killiany, 2012; Hara et al., 2013; Schonheit et al., 2004; West et al., 2004).

We recently published a pathologic validation of the EADC-ADNI HarP (Apostolova et al., 2015). Hippocampal volumes measured using HarP, were significantly correlated with the severity of AD pathology such as neuronal counts, tau and Aβ burden. We also found significant associations between hippocampal volume and Aβ burden in the CA1 and subiculum, tau burden in CA2 and CA3 and neuronal counts in CA1 and CA4.

The present study extends our previous validation work using the EADC-ADNI HarP by investigating the imaging-pathologic correlations in 3D using hippocampal radial distance methodology. We predicted that AD subjects would show greater atrophy of the hippocampus with most significant involvement of the subiculum and CA1 subfields. We hypothesized that neuronal count and tau burden will show stronger associations with hippocampal radial distance relative to Aβ.

2. Material & methods

2.1. Subjects

The study cohort has been previously described (Apostolova et al., 2015). The autopsy brains belonged to the University of California, Los Angeles Alzheimer's Disease Research Center (ADRC) brain bank. The ADRC neuropathology core was funded by the National Institute on Aging (NIA) P50 grant (NIA P50 AG16570). Subjects were 10 AD (6 male, 4 female) and 7 NC (1 male, 6 female) adults without stroke or other gross abnormalities in the temporal lobe and surrounding regions. The Human Research Protection Program (HRPP) and Institutional Review Board (IRB) at the University of California, Los Angeles consider a human subject to be a living individual about whom an investigator obtains data. The current study, which used postmortem tissue, was therefore IRB exempt. All NC subjects died of non-neurological causes and did not have any history of cognitive decline. The autopsy brains were weighed immediately after removal and placed in 10% neutral buffered formalin for at least 10 days. They were then dissected and multiple cortical and subcortical sites sampled and stained for pathologic diagnosis per our local autopsy protocol. One temporal lobe, including the hippocampus, was excised for imaging.

2.2. Imaging analyses

The temporal lobes were scanned post-mortem using a 7 T Bruker Biospec MRI scanner with the following protocol: rapid acquisition with relaxation enhancement (RARE) time to repetition (TR) 1000 ms, time to echo (TE) 80.3 ms, flip angle of 180°, NEX 24, matrix $1024 \times 475 \times 256$, field of view (FOV) $10 \times 6 \times 5$ cm. Three 20-h acquisitions were averaged, resulting in a final resolution of $1.25 \times 1.25 \times 0.195$ mm.

We selected one cognitively normal subject with optimal gray/white matter signal-to-noise ratio as the reference and co-registered the remaining hippocampal scans to this specimen using the Display and Register software package (www.bic.mni.mcgill.ca/software/Display/Display.html) as previously described (Apostolova et al., 2015). Hippocampal structures were manually traced by an expert following HarP protocol and using MultiTracer software created by the Laboratory of NeuroImaging (LONI) at the University of California, Los Angeles, Los Angeles, CA, USA (air.bmap.ucla.edu/MultiTracer). The traces were converted into 3D mesh models and the central core of each hippocampal structure was derived. The radial distance, or the distance from the central core to each surface point, was calculated at each 3D coordinate location of the hippocampal mesh models.

2.3. Pathology analyses

Pathologic diagnosis of AD was determined based on Braak and Braak (Braak and Braak, 1991) and Consortium to Establish and Registry for AD (CERAD) pathologic criteria (1991). The temporal lobes were sectioned coronally into 5 mm slabs, embedded in paraffin from which 6 sections were cut (Zarow et al., 2005). The tissue was stained with cresyl violet, hematoxylin and eosin, Aβ1–40 antibody (AB5074 P, EMD Millipore Corporation, Billerica, USA), and tau antibody (MN1020, Thermo Fisher Scientific Pierce, Rockford, IL, USA). To then visualize the immunostaining, horseradish peroxidase-linked secondary antibodies (Vector MP7401 and MP7402, Vector Laboratories, Burlingame, CA, USA) and 3,3′-diaminobenzidine Peroxidase Substrate Kit (Vector SK-4100, Vector Laboratories, Burlingame, CA, USA) were used as previously described.

Hippocampal subfields (CA1, CA2, CA3, CA4, and subicular pyr-

Table 1
Subject demographics.

Variable	Controls (N = 7)	AD (N = 9)	p-value
Age, years (SD) [Range]	63 (23) [23–85]	82 (8) [70–96]	0.101
Gender (M/F)	6/1	4/5	0.145
Braak and Braak stage	3 I–II	2V	0.01*
	2 III	7 VI	
	2 IV		
Fresh brain weight, g (SD) [Range]	1286 (63) [1210–1400]	1090 (155) [920–1350]	0.039*
Hippocampal volume, mm³ (SD) [Range]	2837 (427) [2241–3405]	1867 (532) [1081–2720]	0.007*

* *p*-value < 0.05.

amidal cell layer) were manually outlined on each slice using the Aperio ImageScope® CS as previously described (Apostolova et al., 2015). Amyloid and tau burden in each subfield were determined with Aperio Positive Pixel Count Algorithm. Neuronal counts were determined using the Aperio IHC Nuclear Image Analysis algorithm followed by visual inspection and manual correction of mislabeled nuclei.

2.4. Statistical analyses

We calculated univariate statistics for imaging and pathologic variables as previously described (Apostolova et al., 2015). We removed subjects whose measures fell 2 standard deviations (SD) from the group mean. Continuous variables were compared using Mann-Whitney *U* test and categorical variables were compared using Fisher exact test. Braak and Braak staging was compared with chi-square testing. Subject demographics are displayed in Table 1.

Radial distance maps were used for statistical analyses with imaging data (see Fig. 1). We used multiple linear regression, designating hippocampal radial distance as the dependent variable, and diagnosis and imaging outcomes (neuronal count, tau and Aβ immunohistochemistry) as independent variables. Independent point-wise regressions were calculated for the 3D images and *p*-values were assigned at every surface point. We conducted type I error correction by statistically permuting the predictor variable (i.e., pathology index) while iteratively testing the global significance of the maps in each experiment. We applied 100,000 permutations to each comparison and derived a single global corrected *p*-value which reflected how often our results might occur by chance alone.

3. Results

Analyses were done with 9 AD and 7 NC (Apostolova et al., 2015). There were no significant differences in age or gender distributions between AD and NC groups. As expected fresh brain weight and hippocampal volume were significantly lower in AD subjects. We excluded one outlier AD male subject from our analyses because his hippocampal volume (4887 mm³) was 4.8 SD from the mean of the NC group.

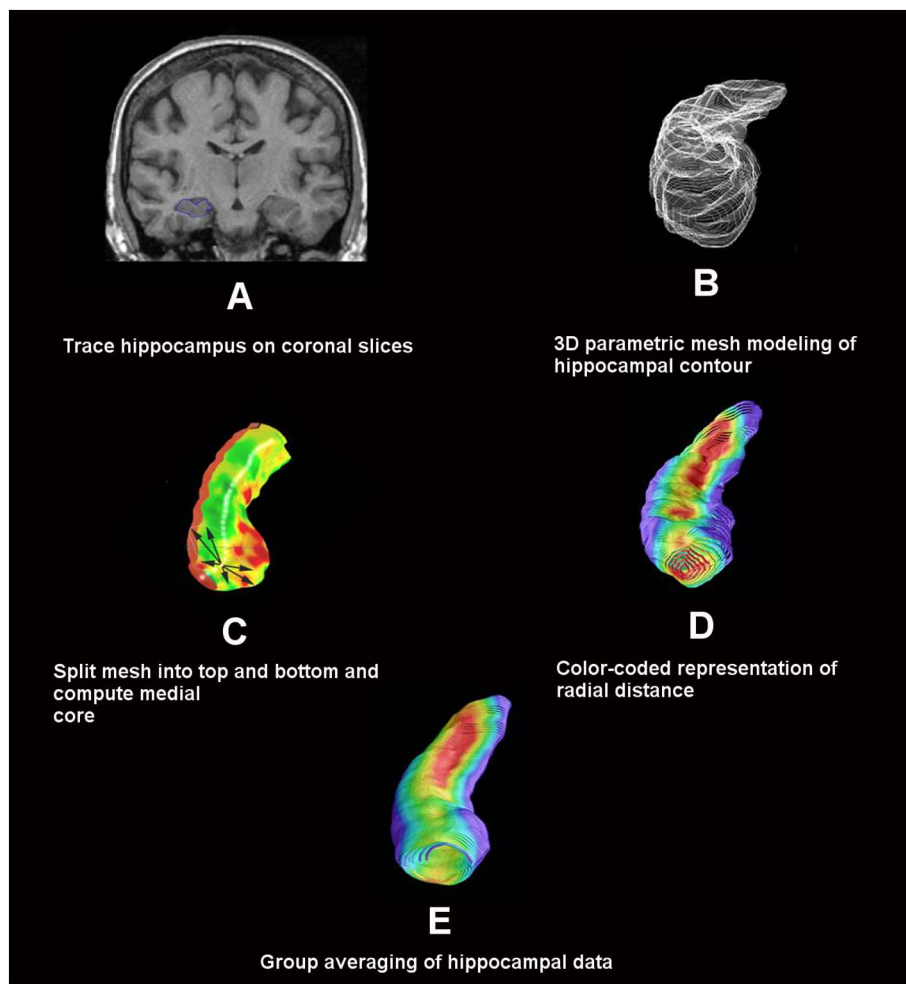Statistical maps from the 3D hippocampal radial distance analyses

A Trace hippocampus on coronal slices

B 3D parametric mesh modeling of hippocampal contour

C Split mesh into top and bottom and compute medial core

D Color-coded representation of radial distance

E Group averaging of hippocampal data

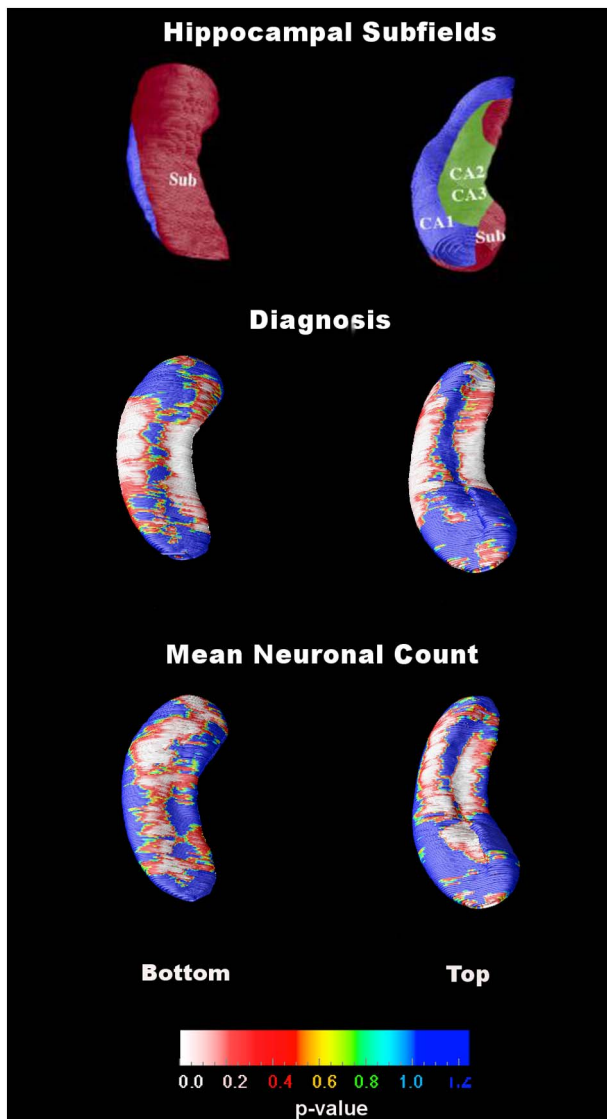**Fig. 1.** Radial distance mapping technique.

Fig. 2. Statistical maps showing the associations of diagnosis (middle row) and mean neuronal count (bottom row) with hippocampal radial distance. The top row images show a schematic representation of the hippocampal subfields mapped onto the hippocampal surface. The subfield definitions are based on work by Duvernoy, Mai and West and Gundersen (Duvernoy, 1988; Mai et al., 2003; West and Gundersen, 1990).

are shown in Fig. 2 and Fig. 3. Hippocampal radial distance was significantly associated with clinical (i.e., premortem) diagnosis ($p < 0.001$). As expected, 3D statistical maps suggested greater hippocampal atrophy in AD subjects than in the NC group. A significant negative association between mean total hippocampal neuronal count and hippocampal radial distance was observed; lower neuron count was indicative of greater hippocampal atrophy ($p = 0.005$). The associations between mean total Abeta and tau burden and hippocampal radial distance were not significant.

Next in our exploratory analyses we investigated how subfield pathology burden estimates relate to hippocampal atrophy measured with the radial distance method. We found a positive association between subicular neuronal count and hippocampal radial distance (i.e., the lower the neuronal counts the lower the radial distance; $p = 0.04$). We also observed a positive association between CA1 neuronal count in CA1 and hippocampal atrophy ($p = 0.07$). There was a negative association between hippocampal radial distance and CA2 tau burden (i.e., the higher the tau burden the lower the radial distance; $p = 0.04$). No associations with Aβ burden were found. Since we do not have the ability to accurately disambiguate the individual
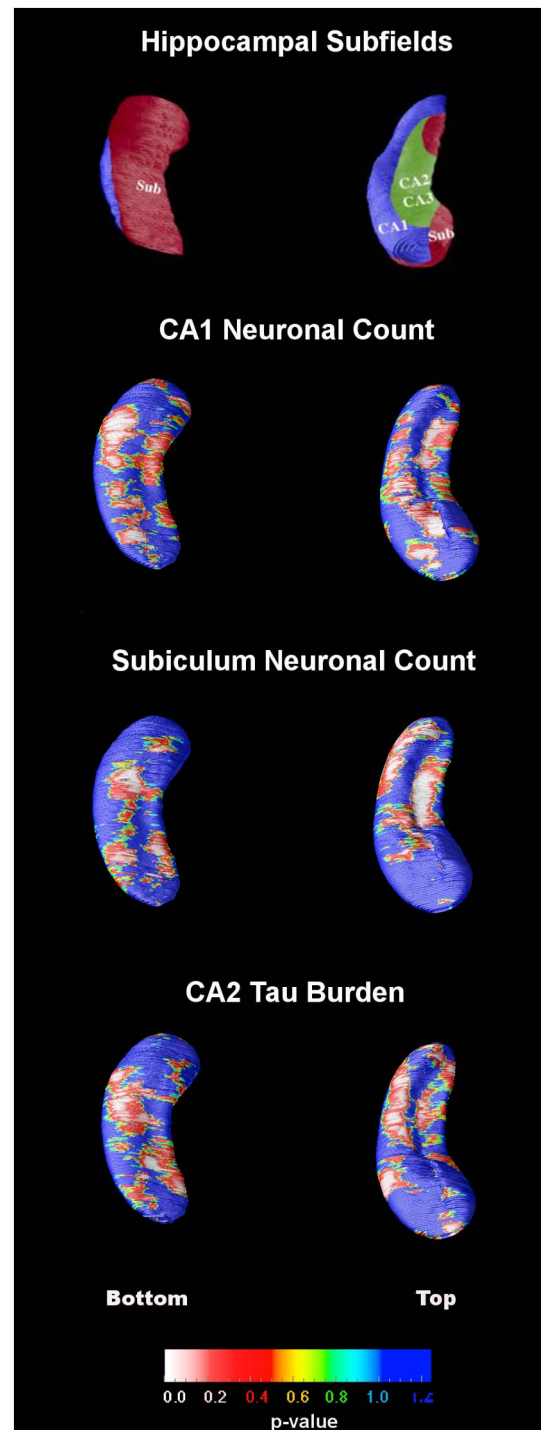

Fig. 3. Statistical maps for subregional hippocampal radial distance associations. The top row images show a schematic representation of the hippocampal subfields mapped onto the hippocampal surface. The subfield definitions are based on work by Duvernoy, Mai and West and Gundersen (Duvernoy, 1988; Mai et al., 2003; West and Gundersen, 1990).

hippocampal subfields, even at 7 T with scanning time as long as 60 h, we were not able to conduct within-subfield correlations of pathology burden and mean radial distance. What we describe are significant associations in the areas of surface projection of these subfields regional associations, as we, and others, have done in the past (Apostolova et al. 2006a; Apostolova et al., 2006c; Apostolova et al., 2010a; Apostolova et al., 2010b; Csernansky et al., 2005; Wang et al., 2003) and also because these exploratory results would not survive correction for multiple comparisons. To that end we have included a schematic

representation of the hippocampal subfields mapped onto the hippocampal surface in Fig. 3. These definitions are based on work by Duvernoy, Mai and West and Gundersen (Duvernoy, 1988; Mai et al., 2003; West and Gundersen, 1990). One can easily appreciate from inspecting the maps in Fig. 3 that the subfield-specific pathologic indices (i.e., subicular and CA1 neuronal count, and CA2 tau burden) showed associations with hippocampal radial distance throughout the hippocampus. This is not unexpected as in AD all hippocampal subfields succumb to atrophy and should thus correlate with pathology severity.

4. Discussion

The development of hippocampal segmentation and morphology analyses has been critically important for the progression of AD research. Despite evidence that the hippocampal subregions uniquely contribute to cognitive processes (Kesner et al., 2004), and are differentially affected by AD pathology over time (Hara et al., 2013; West et al., 2004), most dementia experts treat the hippocampus as a single entity. Here we applied an advanced computational anatomy surface-based approach to study the regional changes in hippocampal shape in AD and validate the radial distance methodology.

As expected, hippocampal atrophy was strongly associated with AD diagnosis (Fig. 2 middle) and neuronal loss (Fig. 2 bottom). The most pronounced associations spanned the locations corresponding to the CA1 and subiculum subfields, which are thought to be the earliest and most severely affected subfields in AD (Schonheit et al., 2004; West et al., 2004). Atrophy in these two subfields is most predictive of future conversion from NC to MCI and from MCI to dementia (Apostolova et al., 2006c; Apostolova et al., 2010a; Apostolova et al., 2010b).

In our previously published hippocampal volumetric analyses (Apostolova et al., 2015) we reported significant associations between CA1 and subicular neuronal counts and mean hippocampal volume. Thus the associations of CA1 and subicular neuronal counts with hippocampal radial distance are in line with our expectations. In our volumetric study we also found significant associations CA2 and CA3 tau burden and hippocampal volume. Here we observe significant association between hippocampal radial distance and tau burden in the CA2 subfield only. Unlike our volumetric pathologic validation study, we did not find significant associations between Aβ burden and hippocampal radial distance. This is likely due to the fact that radial distance reflects atrophy as a distributed thickness difference across the full extent of the hippocampal structure, which could be more powerful way to detect strong localized effects but not weak widely distributed effects.

As mentioned in the results section, the subfield-specific pathologic indices did not show circumscribed regional effect, but rather a widespread association with hippocampal radial distance. This is not unexpected as in AD all hippocampal subfields succumb to atrophy, and would thus correlate with pathology severity measured from the whole hippocampus or from a given subfield. In other words, AD subjects will have higher global and regional pathology burden and widely distributed hippocampal atrophy and these measures will be expected to correlate with each other.

There are several strengths and weaknesses of this study. The study is limited by its small sample size. The autopsy cases at UCLA might not adequately represent the US population. Regardless of that, we found the expected associations of hippocampal AD pathology indices with radial distance. Yet given the small sample size, the findings from our study should be further validated in other cohorts. A major strength of this study is the use of 7 T imaging on post mortem tissue. 7 T imaging has the advantage of improved resolution and reduced signal-to-noise ratio, which allows for greater precision and consistency in our methodology and analyses when compared to the currently available in vivo imaging techniques.

5. Conclusion

The associations shown here between hippocampal radial distance and pathological variables using HarP as a hippocampal segmentation tool provide support for the use of hippocampal surface mapping in AD research. The findings reported here provide further pathological validation for both the use of hippocampal radial distance as a measure of neuropathologic effects of AD, and development of digital hippocampal segmentation using the HarP method in order to distinguish specific hippocampal subfields and improve the current standards for hippocampal segmentation.

References

Apostolova, L., Dinov, I., Dutton, R.A., Hayashi, K.M., Toga, A.W., Cummings, J.L., Thompson, P.M., 2006a. 3D comparison of hippocampal atrophy in amnestic mild cognitive impairment and Alzheimer's disease. Brain 129, 2867–2873.

Apostolova, L.G., Dinov, I.D., Dutton, R.A., Hayashi, K.M., Toga, A.W., Cummings, J.L., Thompson, P.M., 2006b. 3D comparison of hippocampal atrophy in amnestic mild cognitive impairment and Alzheimer's disease. Brain 129, 2867–2873.

Apostolova, L.G., Dutton, R.A., Dinov, I.D., Hayashi, K.M., Toga, A.W., Cummings, J.L., Thompson, P.M., 2006c. Conversion of mild cognitive impairment to Alzheimer disease predicted by hippocampal atrophy maps. Arch. Neurol. 63, 693–699.

Apostolova, L.G., Mosconi, L., Thompson, P.M., Green, A.E., Hwang, K.S., Ramirez, A., Mistur, R., Tsui, W.H., de Leon, M.J., 2010a. Subregional hippocampal atrophy predicts Alzheimer's dementia in the cognitively normal. Neurobiol. Aging 31, 1077–1088.

Apostolova, L.G., Thompson, P.M., Green, A.E., Hwang, K.S., Zoumalan, C., Jack Jr., C.R., Harvey, D.J., Petersen, R.C., Thal, L.J., Aisen, P.S., Toga, A.W., Cummings, J.L., Decarli, C.S., 2010b. 3D comparison of low, intermediate, and advanced hippocampal atrophy in MCI. Hum. Brain Mapp. 31, 786–797.

Apostolova, L.G., Green, A.E., Babakchanian, S., Hwang, K.S., Chou, Y.Y., Toga, A.W., Thompson, P.M., 2012. Hippocampal atrophy and ventricular enlargement in normal aging, mild cognitive impairment (MCI), and Alzheimer disease. Alzheimer Dis. Assoc. Disord. 26, 17–27.

Apostolova, L.G., Zarow, C., Biado, K., Hurtz, S., Boccardi, M., Somme, J., Honarpisheh, H., Blanken, A.E., Brook, J., Tung, S., Lo, D., Ng, D., Alger, J.R., Vinters, H.V., Bocchetta, M., Duvernoy, H., Jack Jr., C.R., Frisoni, G.B., 2015. Relationship between hippocampal atrophy and neuropathology markers: a 7T MRI validation study of the EADC-ADNI harmonized hippocampal segmentation protocol. Alzheimers Dement. 11, 139–150.

Arnold, S.E., Hyman, B.T., Flory, J., Damasio, A.R., Van Hoesen, G.W., 1991. The topographical and neuroanatomical distribution of neurofibrillary tangles and neuritic plaques in the cerebral cortex of patients with Alzheimer's disease. Cereb. Cortex 1, 103–116.

Beach, T.G., Monsell, S.E., Phillips, L.E., Kukull, W., 2012. Accuracy of the clinical diagnosis of Alzheimer disease at National Institute on Aging Alzheimer Disease Centers, 2005–2010. J. Neuropathol. Exp. Neurol. 71, 266–273.

Bobinski, M., Wegiel, J., Wisniewski, H.M., Tarnawski, M., Reisberg, B., Mlodzik, B., de Leon, M.J., Miller, D.C., 1995. Atrophy of hippocampal formation subdivisions correlates with stage and duration of Alzheimer disease. Dementia 6, 205–210.

Boccardi, M., Ganzola, R., Bocchetta, M., Pievani, M., Redolfi, A., Bartzokis, G., Camicioli, R., Csernansky, J.G., de Leon, M.J., deToledo-Morrell, L., Killiany, R.J., Lehericy, S., Pantel, J., Pruessner, J.C., Soininen, H., Watson, C., Duchesne, S., Jack Jr., C.R., Frisoni, G.B., 2011. Survey of protocols for the manual segmentation of the hippocampus: preparatory steps towards a joint EADC-ADNI harmonized protocol. J. Alzheimers Dis. 26 (Suppl. 3), 61–75.

Boccardi, M., Bocchetta, M., Apostolova, L.G., Preboske, G., Robitaille, N., Pasqualetti, P., Collins, L.D., Duchesne, S., Jack Jr., C.R., Frisoni, G.B., 2014. Establishing magnetic resonance images orientation for the EADC-ADNI manual hippocampal segmentation protocol. J. Neuroimaging 24, 509–514.

Boccardi, M., Bocchetta, M., Apostolova, L.G., Barnes, J., Bartzokis, G., Corbetta, G., DeCarli, C., deToledo-Morrell, L., Firbank, M., Ganzola, R., Gerritsen, L., Henneman, W., Killiany, R.J., Malykhin, N., Pasqualetti, P., Pruessner, J.C., Redolfi, A., Robitaille, N., Soininen, H., Tolomeo, D., Wang, L., Watson, C., Wolf, H., Duvernoy, H., Duchesne, S., Jack Jr., C.R., Frisoni, G.B., 2015. Delphi definition of the EADC-ADNI harmonized protocol for hippocampal segmentation on magnetic resonance. Alzheimers Dement. 11, 126–138.

Bocchetta, M., Boccardi, M., Ganzola, R., Apostolova, L.G., Preboske, G., Wolf, D., Ferrari, C., Pasqualetti, P., Robitaille, N., Duchesne, S., Jack Jr., C.R., Frisoni, G.B., 2015.

Harmonized benchmark labels of the hippocampus on magnetic resonance: the EADC-ADNI project. Alzheimers Dement. 11, 151–160 e155.

Braak, H., Braak, E., 1991. Neuropathological stageing of Alzheimer-related changes. Acta Neuropathol. 82, 239–259.

Braak, H., Braak, E., 1997. Staging of Alzheimer-related cortical destruction. Int. Psychogeriatr. 9 (Suppl. 1), 257–261 (discussion 269-272).

Csernansky, J.G., Wang, L., Swank, J., Miller, J.P., Gado, M., McKeel, D., Miller, M.I., Morris, J.C., 2005. Preclinical detection of Alzheimer's disease: hippocampal shape and volume predict dementia onset in the elderly. NeuroImage 25, 783–792.

Duchesne, S., Valdivia, F., Robitaille, N., Mouiha, A., Valdivia, F.A., Bocchetta, M., Apostolova, L.G., Ganzola, R., Preboske, G., Wolf, D., Boccardi, M., Jack Jr., C.R., Frisoni, G.B., 2015. Manual segmentation qualification platform for the EADC-ADNI harmonized protocol for hippocampal segmentation project. Alzheimers Dement. 11, 161–174.

Duvernoy, H.M., 1988. The Human Hippocampus — An Atlas of Applied Anatomy | Henri M. Duvernoy | Springer, 1 ed. J.F. Bergman-Verlag Munchen, Munich.

Frisoni, G.B., Jack, C.R., 2011. Harmonization of magnetic resonance-based manual hippocampal segmentation: a mandatory step for wide clinical use. Alzheimers Dement. 7, 171–174.

Frisoni, G.B., Sabattoli, F., Lee, A.D., Dutton, R.A., Toga, A.W., Thompson, P.M., 2006. In vivo neuropathology of the hippocampal formation in AD: a radial mapping MR-based study. NeuroImage 32, 104–110.

Frisoni, G.B., Jack Jr., C.R., Bocchetta, M., Bauer, C., Frederiksen, K.S., Liu, Y., Preboske, G., Swihart, T., Blair, M., Cavedo, E., Grothe, M.J., Lanfredi, M., Martinez, O., Nishikawa, M., Portegies, M., Stoub, T., Ward, C., Apostolova, L.G., Ganzola, R., Wolf, D., Barkhof, F., Bartzokis, G., DeCarli, C., Csernansky, J.G., deToledo-Morrell, L., Geerlings, M.I., Kaye, J., Killiany, R.J., Lehericy, S., Matsuda, H., O'Brien, J., Silbert, L.C., Scheltens, P., Soininen, H., Teipel, S., Waldemar, G., Fellgiebel, A., Barnes, J., Firbank, M., Gerritsen, L., Henneman, W., Malykhin, N., Pruessner, J.C., Wang, L., Watson, C., Wolf, H., deLeon, M., Pantel, J., Ferrari, C., Bosco, P., Pasqualetti, P., Duchesne, S., Duvernoy, H., Boccardi, M., 2015. The EADC-ADNI harmonized protocol for manual hippocampal segmentation on magnetic resonance: evidence of validity. Alzheimers Dement. 11, 111–125.

Greene, S.J., Killiany, R.J., 2012. Hippocampal subregions are differentially affected in the progression to Alzheimer's disease. Anat Rec (Hoboken) 295, 132–140.

Hara, M., Hirokawa, K., Kamei, S., Uchihara, T., 2013. Isoform transition from four-repeat to three-repeat tau underlies dendrosomatic and regional progression of neurofibrillary pathology. Acta Neuropathol. 125, 565–579.

Hof, P.R., Glannakopoulos, P., Bouras, C., 1996. The neuropathological changes associated with normal brain aging. Histol. Histopathol. 11, 1075–1088.

Jack Jr., C.R., Dickson, D.W., Parisi, J.E., Xu, Y.C., Cha, R.H., O'Brien, P.C., Edland, S.D.,

Smith, G.E., Boeve, B.F., Tangalos, E.G., Kokmen, E., Petersen, R.C., 2002. Antemortem MRI findings correlate with hippocampal neuropathology in typical aging and dementia. Neurology 58, 750–757.

Kesner, R.P., Lee, I., Gilbert, P., 2004. A behavioral assessment of hippocampal function based on a subregional analysis. Rev. Neurosci. 15, 333–351.

Mai, J.K.P., Assheuer, G., Joseph, K., 2003. Atlas of the Human Brain, second ed. Elsevier Academic Press, San Diego, CA.

Morra, J.H., Tu, Z., Apostolova, L.G., Green, A.E., Avedissian, C., Madsen, S.K., Parikshak, N., Toga, A.W., Jack Jr., C.R., Schuff, N., Weiner, M.W., Thompson, P.M., 2009. Automated mapping of hippocampal atrophy in 1-year repeat MRI data from 490 subjects with Alzheimer's disease, mild cognitive impairment, and elderly controls. NeuroImage 45, S3–15.

Nelson, P.T., Alafuzoff, I., Bigio, E.H., Bouras, C., Braak, H., Cairns, N.J., Castellani, R.J., Crain, B.J., Davies, P., Del Tredici, K., Duyckaerts, C., Frosch, M.P., Haroutunian, V., Hof, P.R., Hulette, C.M., Hyman, B.T., Iwatsubo, T., Jellinger, K.A., Jicha, G.A., Kovari, E., Kukull, W.A., Leverenz, J.B., Love, S., Mackenzie, I.R., Mann, D.M., Masliah, E., McKee, A.C., Montine, T.J., Morris, J.C., Schneider, J.A., Sonnen, J.A., Thal, D.R., Trojanowski, J.Q., Troncoso, J.C., Wisniewski, T., Woltjer, R.L., Beach, T.G., 2012. Correlation of Alzheimer disease neuropathologic changes with cognitive status: a review of the literature. J. Neuropathol. Exp. Neurol. 71, 362–381.

Schonheit, B., Zarski, R., Ohm, T.G., 2004. Spatial and temporal relationships between plaques and tangles in Alzheimer-pathology. Neurobiol. Aging 25, 697–711.

Shim, Y.S., Roe, C.M., Buckles, V.D., Morris, J.C., 2013. Clinicopathologic study of Alzheimer's disease: Alzheimer mimics. J. Alzheimers Dis. 35, 799–811.

Thal, D.R., Rub, U., Schultz, C., Sassin, I., Ghebremedhin, E., Del Tredici, K., Braak, E., Braak, H., 2000. Sequence of Abeta-protein deposition in the human medial temporal lobe. J. Neuropathol. Exp. Neurol. 59, 733–748.

Thompson, P.M., Hayashi, K.M., De Zubicaray, G.I., Janke, A.L., Rose, S.E., Semple, J., Hong, M.S., Herman, D.H., Gravano, D., Doddrell, D.M., Toga, A.W., 2004. Mapping hippocampal and ventricular change in Alzheimer disease. NeuroImage 22, 1754–1766.

Wang, L., Swank, J.S., Glick, I.E., Gado, M.H., Miller, M.I., Morris, J.C., Csernansky, J.G., 2003. Changes in hippocampal volume and shape across time distinguish dementia of the Alzheimer type from healthy aging. NeuroImage 20, 667–682.

West, M.J., Gundersen, H.J., 1990. Unbiased stereological estimation of the number of neurons in the human hippocampus. J. Comp. Neurol. 296, 1–22.

West, M.J., Kawas, C.H., Stewart, W.F., Rudow, G.L., Troncoso, J.C., 2004. Hippocampal neurons in pre-clinical Alzheimer's disease. Neurobiol. Aging 25, 1205–1212.

Zarow, C., Vinters, H.V., Ellis, W.G., Weiner, M.W., Mungas, D., White, L., Chui, H.C., 2005. Correlates of hippocampal neuron number in Alzheimer's disease and ischemic vascular dementia. Ann. Neurol. 57, 896–903.